A Search for Hard X-Ray Emission from Globular Clusters - Constraints from BATSE

E. Ford[1], P. Kaaret[1], B.A. Harmon[2], M. Tavani[1], and S.N. Zhang[3]

ABSTRACT

We have monitored a sample of 27 nearby globular clusters in the hard X-ray band ($20-120$ keV) for $\sim$1400 days using the BATSE instrument on board the Compton Gamma-Ray Observatory. Globular clusters may contain a large number of compact objects (e.g., pulsars or X-ray binaries containing neutron stars) which can produce hard X-ray emission. Our search provides a sensitive ($\sim$50 mCrab) monitor for hard X-ray transient events on time scales of $\gtrsim 1$ day and a means for observing persistent hard X-ray emission. We have discovered no transient events from any of the clusters and no persistent emission. Our observations include a sensitive search of four nearby clusters containing dim X-ray sources: 47 Tucanae, NGC 5139, NGC 6397, and NGC 6752. The non-detection in these clusters implies a lower limit for the recurrence time of transients of 2 to 6 years for events with luminosities $\gtrsim 10^{36}$ erg s^{-1} ($20-120$ keV) and $\sim$ 20 years if the sources in these clusters are taken collectively. This suggests that the dim X-ray sources in these clusters are not transients similar to Aql X-1. We also place upper limits on the persistent emission in the range $(2-10)\times 10^{34}$ erg s^{-1} (2σ, $20-120$ keV) for these four clusters. For 47 Tuc the upper limit is more sensitive than previous measurements by a factor of 3. We find a model dependent upper limit of 19 isolated millisecond pulsars (MSPs)

[1]Columbia University, Department of Physics and Columbia Astrophysics Lab, 538 W. 120th Street, New York, NY 10027

[2]NASA/Marshall Space Flight Center, ES 66, Huntsville, AL 35812

[3]University Space Research Association/ MSFC, ES 66, Huntsville, AL 35812

producing gamma-rays in 47 Tuc, compared to the 11 observed radio MSPs in this cluster.

Subject headings: clusters:globular, 47 Tucanae, NGC 5139, NGC 6752, NGC 6397, X-ray:transients

1. Introduction

Globular clusters (GCs) are remarkable stellar systems where a variety of compact objects may form and evolve. Numerous millisecond pulsars (MSPs) inhabit GCs as revealed by radio observations (Lyne 1996), e.g. 11 MSPs in 47 Tuc (Robinson et al. 1995). In the X-ray band, the number of bright sources ($1 - 10$ keV) per unit stellar mass is two orders of magnitude larger for GCs than for the remainder of the galaxy (Clark 1975). Persistent X-ray sources in GCs divide into two luminosity groups: one with low luminosities ($L_x \lesssim 10^{34.5}$ erg s^{-1}, $0.5 - 4.5$ keV), and the other with high luminosities ($L_x \gtrsim 10^{36}$ erg s^{-1}) (Hertz and Grindlay 1983, Hertz and Wood 1985, Verbunt et al. 1995). The nature of the low luminosity, dim X-ray sources (DXSs) has been controversial (for reviews see Bailyn 1995, Verbunt et al. 1994, Grindlay 1993b, Hut et al. 1992). Suggestions for their origin include cataclysmic variables, with mass accreting onto a white dwarf (Grindlay 1993a), low mass X-ray binaries (LMXBs) with accretion at quiescent levels onto a neutron star (NS) or black hole (BH) (Verbunt, Van Paradijs and Elson 1984), plerionic MSP binaries (Tavani 1991) or chance superpositions of foreground/background objects (Margon and Bolte 1987).

We have employed the BATSE instrument on board the Compton Gamma-Ray Observatory to search for transient and persistent hard X-ray emission ($\gtrsim$ 20 keV). Hard X-rays may be produced by GC compact objects in a number of ways. In a binary, hard X-ray emission can be powered by mass accretion onto the BH/NS primary, or in pulsars, from shock interactions in the relativistic pulsar winds in the binary. Hard X-ray emission may also be produced by magnetospheric emission of isolated MSPs. Transient emission has been observed previously from GCs. NGC 6440, a GC containing DXSs, has exhibited a high luminosity transient episode (Forman, Jones and Tananbaum 1976). M15 may also have shown a transient event (Pye and McHardy 1983). In the hard X-ray band, SIGMA has observed transient emission from the globular cluster Terzan 2. Recent ROSAT HRI observations indicate that the SIGMA source is most likely associated with the X-ray burster XB 1724-30 (Mereghetti et al. 1995). SLX 1732-304 in the GC Terzan 1 has also been detected as a hard X-ray source (Churazov et al. 1994). Our search does not include Terzan 2, Terzan 1 or NGC 6440 due to problems with nearby interfering sources. We have been able to observe M15 however.

In Section 2, we describe hard X-ray emission mechanisms in detail. Section 3 outlines the BATSE earth occultation flux measurement technique and the parameters of our search. In Sections 4 and 5 we present the results of our search, providing upper limits on transient events and constraints on the recurrence times of transients from DXSs. Section 6 contains upper limits on persistent emission and constraints on the number of isolated and interacting MSPs. Section 7 is a summary and conclusion.

2. Hard X-ray emission from compact objects

2.1. Accreting black holes

Soft X-ray transients (SXTs) have exhibited emission in excess of 10 keV (e.g. White, Kaluzienski and Swank 1984). These hard power law tails along with an anticorrelation of intensity and spectral hardness have been taken as indications of a BH primary (Tanaka

1989, Tanaka and Lewin 1995).

Originally, the discovery of X-ray sources in GCs was interpreted as a possible manifestation of massive accreting BHs (e.g., Bahcall and Ostriker 1975). We know today that *all* bright X-ray sources in GCs show X-ray bursts, and therefore most likely contain neutron stars. Though it is unlikely that clusters contain very massive black holes, they may harbor a population of stellar mass black holes. Kulkarni, Hut and McMillan (1993) estimate that there may be ~ 10 systems in galactic GCs in which a BH of mass $\sim 10 M_\odot$ has captured a companion. In a few of these systems the companion may have had time to evolve off the main sequence, producing an active X-ray binary. Hard X-ray activity from such systems would be observable in our search.

2.2. Accreting neutron stars

LMXBs that contain NS primaries and accrete with luminosities below some critical value also exhibit transient episodes of hard X-ray emission (e.g. Barret and Vedrenne 1994) and an anticorrelation of spectral hardness and intensity, e.g.: 4U0614+091 (Barret and Grindlay 1995a), 4U1608-522 (Mitsuda et al. 1989).

Table 1 lists the observed hard X-ray properties of several transient and persistent LMXBs. All of these sources have been observed as type-I X-ray bursters which indicate NS primaries. The hard X-ray outbursts generally exceed 10^{36} erg s^{-1}, with emission extending above 100 keV. The time scales for the hard X-ray outbursts are typically $10 - 100$ days. Such events would be easily detectable in our search. Additional bursters are being detected as hard X-ray sources in a BATSE monitoring program (Barret et al. 1996).

2.3. Isolated and binary Pulsars

Persistent hard X-ray emission may also be produced by MSPs, and the fact that GCs contain large numbers of MSPs makes them ideal systems in which to search for such emission (Chen 1991, Tavani 1993b). Recent theoretical work has shown that hard X-ray and gamma ray emission may be produced by MSPs either in isolation (Chen, Middleditch and Ruderman 1993) or in interacting binaries (Tavani 1993a). Isolated MSPs could produce hard X-ray emission by the same mechanism operating in young Crab-like pulsars. Though the magnetic fields are smaller in recycled pulsars, the voltage drop at the light cylinder may be similar due to the smaller rotation periods (Ruderman and Cheng 1988). In binary systems, MSPs may emit hard X-rays by interaction with a companion (Tavani 1991). This is in analogy to PSR B1957+20 in which the pulsar is evaporating its companion (e.g. Kluzniak et al. 1988). In such systems the pulsar is partly or fully buried in a gaseous envelope originating from its companion. The interaction of the MSP wind with the surrounding material produces energetic emission by synchrotron radiation or inverse Compton scattering of shock accelerated particles. Emission, which can be explained by this model, has recently been observed in the $1 - 200$ keV range from the binary pulsar PSR 1259-63 near periastron (Grove et al. 1995, Tavani et al. 1996).

3. Cluster Search with BATSE

The BATSE instrument was designed to provide continuous coverage of the entire sky in the hard X-ray/gamma-ray band from 20 keV $-$ 2 MeV (Harmon et al. 1992), and has an optimal sensitivity in the range $20 - 120$ keV

Source	D (kpc)	L_x (erg s^{-1})	Observation
Aql X-1	2.5	1×10^{36}	BATSE $(20-120$ keV)[a]
Cen X-4	1.2	7×10^{36}	Signe 2MP $(13-163$ keV) [b]
XB 1724-308 (Ter 2)	14.0	2×10^{37}	SIGMA $(35-200$ keV) [c]
KS1731-260	8.5	2×10^{37}	SIGMA [d]
4U1608-522	3.6	6×10^{36}	BATSE[e]
A1742-294	8.5	6×10^{36}	SIGMA[f]

Table 1: Hard X-ray outburst luminosities of five X-ray bursters. L_x is the peak outburst luminosity for the $20-120$ keV band. The energy bands of each instrument are shown.

[a](Harmon et al. 1996)
[b](Bouchacourt et al. 1984)
[c](Barret et al. 1991)
[d](Barret et al. 1992)
[e](Zhang et al. 1996)
[f](Churazov et al. 1995)

for a source with a typical photon index of 2. Source fluxes are measured by BATSE using the earth as an occulting object. As a source rises or sets, steps appears in the detector count rates due to attenuation by the Earth's atmosphere. Source fluxes are determined by fitting the amplitude of these steps. Thus, depending on the geometry of the Earth's rising and setting limbs, one can make two source measurements per GRO orbit (approximately 90 min.), and from these construct a light curve.

Fluxes in the resulting light curve, for a location in the sky with no sources, form a distribution about a mean flux of zero. Both positive and negative fluxes are produced in the occultation edge fits, all with formal error estimates. The distribution of flux estimates has a width which is larger than expected for a Poisson distribution of background rates. This is due to systematic effects, such as contributions in the occultation fits from nearby sources and spurious background fluctuations.

The main limitation of the occultation technique is source confusion due to the large angular extent of the Earth's occulting limbs. There are several diagnostics that can be employed to identify confused sources. One such check is to compare the measured relative rates in separate detectors to the rates expected given the BATSE detector responses (Pendleton et al. 1996). Another technique is to compare the rates from the rising limb to those from the setting limb. For constant flux from the expected source, the rising and setting edges should give the same rates. The precession of the earth's limb can also be used to localize the emission, a technique that has been successfully employed to create images of sky regions for brighter, long duration events (Zhang et al. 1993).

We divide our search of 27 GCs into two parts, which we will refer to as Search A

and Search B (see Figure 1a). Search A is a lower sensitivity search of 23 GCs which are at larger distances and/or in regions of the sky prone to source confusion. Search A includes GCs at distances $\lesssim 6$ kpc, GCs near the galactic center, GCs containing no known DXSs, and GCs known to contain bright LMXBs. Search B is a higher sensitivity search of four nearby GCs which are not subject to serious source confusion problems. We limit this search to GCs at $\lesssim 6$ kpc which also contain DXSs near the cluster core. We also exclude clusters within 15^{o} of the galactic center, to avoid source confusion in this dense area. The GCs of Search B are shown in Figure 1b (circled). In what follows, all cluster parameters have been taken from Peterson (1993).

4. Results from Search A

We have generated light curves for all the clusters extending from April 1991 to March 1995 ($\sim$1400 days). For Search A, we have analyzed the rate history of each cluster for events with structure on a time scale of one or more days. Generally in each light curve there are several "events" apparent; most of these can be attributed to interference from nearby bright sources. There are, however, a few spikes that cannot readily be explained as interfering sources. None of these events are particularly outstanding in terms of amplitude or structure. For Search B we have further analyzed such events to determine if they originate from the clusters, as described below. For the 23 clusters in Search A, however, such an analysis is impractical. For Search A, therefore, we take the largest of the outstanding features to set conservative upper limits to the minimum observable event amplitude (Table 2). We initially find count rate upper limits (R_{ul} in Table 2). To convert these limits to photon fluxes, we have multiplied by a constant conversion factor determined from other light curves for which we have properly deconvolved the instrument response with an assumed photon index of 2.0 to generate photon flux histories. This conversion is accurate to within approximately 30%. From the photon rate, we calculate a luminosity upper limit by assuming power law spectra with index 2. The effective time coverage for each cluster is shown in Table 2. Coverage with BATSE is less than 100% and varies as a function of sky position due to the geometry of the Earth's occulting limbs and due to interfering sources. When target occultations occur within 10 seconds of the occultation of a bright interfering source, no edge fits are produced. This leads to data gaps, as in the case of NGC 6760, which has highly non-uniform coverage due to the nearby source Aql X-1. Note that we obtain a limit of $\sim 10^{37}$ erg s^{-1} for NGC 5272 (M3) which is known to contain a time variable supersoft X-ray source. Note also that the cluster NGC 6440 has been excluded from our search due to nearby interfering sources.

5. Results from Search B

For Search B, we have produced rate histories over the time period mentioned above and properly deconvolved the detector response to obtain photon light curves. We have searched these light curves for outburst events. Candidate events are identified as features of duration one or more days which rise at least 1.5σ above the background flux distribution. With this criterion we have identified 40 possible candidate events. We analyzed each of these isolated events further to determine if they originate from the clusters. We check for nearby interfering sources and compare the relative rates in the detectors. This anal-

Cluster	D (kpc)	R_{ul} (cnt s^{-1})	F_{ul} (γ $cm^{-2}s^{-1}$) [$\times 10^{-2}$]	L_{ul} (erg s^{-1}) [$\times 10^{36}$]	coverage (%)	Persistent X-ray Source(s)
M4	2.0	3.5	2.8	0.9	80.0	
NGC6544	2.5	4.0	3.2	1.7	77.1	
NGC6656	3.0	2.6	2.1	1.6	82.4	dim
NGC6838	3.9	4.0	3.2	4.0	80.5	
NGC6539	4.0	4.4	3.5	4.7	70.9	
NGC6366	4.0	6.5	5.2	6.9	74.9	
NGC6760	4.2	6.3	5.0	7.2	38.7	
NGC6254	4.3	3.3	2.6	4.0	74.3	
NGC6809	4.8	4.5	3.6	6.8	72.3	
NGC3201	5.0	7.0	5.6	11.6	77.6	
NGC4372	5.2	4.0	3.2	7.2	69.8	
NGC6218	5.6	3.8	3.0	7.8	74.5	
NGC4833	5.8	2.9	2.3	6.4	69.0	
NGC6626	5.9	4.0	3.2	9.2	79.4	dim
NGC6541	6.6	3.3	2.6	9.3	73.3	dim
NGC6712	6.8	4.4	3.5	13.4	72.9	bright
NGC7099	7.4	3.0	2.4	10.9	88.4	dim
NGC6341	7.5	3.5	2.8	13.0	85.7	dim
NGC6624	8.1	3.5	2.8	15.2	84.2	bright
NGC5272	10.1	2.4	1.9	16.0	88.0	dim
M15	10.5	3.5	2.8	25.5	87.6	bright
NGC1851	12.2	4.5	3.6	44.3	88.1	bright
NGC1904	13.0	3.1	2.5	34.9	88.1	dim

Table 2: Event upper limits and coverage time for the 23 GCs in Search A. R_{ul} is the raw count rate upper limit for hard X-ray transient events, and F_{ul} the approximate corresponding limit in flux units. The luminosity upper limit ($20-120$ keV), L_{ul}, assumes the stated distances and power law spectra with index 2. The total time span is 1630 days for NGC 6544 and NGC 6656 and 1490 days for the other clusters. The clusters containing bright and dim X-ray sources are marked.

ysis eliminates all but 13 of the events as candidates. These 13 candidates consist of peak-like structures with durations of 1 to 8 days. The significance of these events, as measured from the photon flux error bars near the peaks, ranges from 2σ to 6σ. The maximum luminosities in these candidate events would range from $0.7 - 6 \times 10^{36}$ erg s^{-1}, and in one case 9×10^{36} erg s^{-1} $(20 - 120$ keV). These luminosities are similar to the expected transient peak luminosities (c.f. Table 1) and deserve further investigation.

We further analyze candidate events by studying the correlation between the rising and setting rates within a given GRO pointing period. Figures 2a and 2b show example rate histories for candidate events in NGC 6752 and NGC 5139. For each source, the rise and set rates clearly have different temporal behaviors. In each case nearly all the flux is from the fits in the rising limbs. Formally we can calculate the correlation coefficient for the rising vs setting rates. As a test of this technique we have calculated the correlation coefficient for a two day data sample from the Crab. The rise and set data for the Crab are well correlated with a correlation coefficient of 0.77 and a corresponding probability of 2.6% that the observed correlation could arise from a random sample. For the two events shown in Figures 2a and 2b the correlation coefficients are -0.07 and -0.10 respectively, with a 54% and 49% probability of being random. We have calculated the correlation coefficient for the other 11 candidate events during the relevant time intervals. For each event the rises and sets either show very weak correlation or, in several cases, strong anticorrelation. The most significant correlation has a 30.3% probability of being random. The lack of significant positive correlations imply that the "events" observed in the light curves do not originate from the target sources but are due to interfering sources located elsewhere.

As a check to this interpretation we have analyzed the event in NGC 6752 shown in Figure 2a in more depth. We have chosen to look further at this particular event because it is somewhat extended in time, lasting for approximately 5 days, and reaches moderate flux levels. We have produced a map in an approximately $7^o \times 7^o$ region centered on NGC 6752 during the time of the candidate event. The map is created by forming a grid of points separated by 0.5^o, and producing occultation histories for each grid point. The resulting rates for each point can be combined together to form a map. The map for the NGC 6752 event shows an emission enhancement well localized at $\sim 3^o$ 'northeast' of the cluster during the first GRO pointing period (TJD $9078 - 9083$). It is also clear from the limb geometry that such an event would be visible only on the setting rates, and indeed this is what is observed in the rate history for NGC 6752. During the second pointing period (TJD $9083 - 9090$), the emission peak moves to $\sim 1^o$ 'southwest' of the cluster, and is well localized only in the detector with the less optimal pointing. All of this leads us to conclude that the enhancement is not associated with the cluster.

5.1. Recurrence time limits from DXSs

In the absence of any detected transient events, we are able to set a lower limit to the recurrence times of transient sources in the clusters of Search B. For a given time interval in a GC light curve, there will be a minimum luminosity, L_{min}, at which an event would be visible. L_{min} is determined by the width of the flux distribution. We step through the

cluster light curves and determine the total number of days that events of different L_{min}s would be observable. The result is a distribution of the number of days observable vs L_{min} (Figure 3a). The L_{min} distribution depends on the assumed duration of outburst events and the photon index used in the deconvolution. This dependence, however, is rather weak. The distribution depends more strongly on the time intervals into which the data are integrated. Figure 3b shows the L_{min} distribution for different data integration times. The minimum observable luminosities are shifted down at longer integration times due to an increased sensitivity, i.e. a smaller width in the distribution of fluxes.

We determine limits to the recurrence times of outbursts from the L_{min} distribution. For each L_{min} there is an associated observable time, T_{obs}, for which an event exceeding L_{min} would be detectable. T_{obs} is essentially the integral of the L_{min} distribution. T_{obs} is related to the mean event recurrence time, τ_{event}, by $P = e^{-T_{obs}/\tau_{event}}$, where P is the probability of observing no events in time T_{obs} assuming a Poisson distribution of events. We calculate a lower limit for τ_{event} using a 5% probability of detection. With multiple X-ray sources in each cluster, an event could originate from any of the sources. The minimum event recurrence time, τ_{event}, can be stated as a minimum recurrence time for sources, if we use the number of DXSs in each cluster, N_{DXS}. The minimum source recurrence time, τ_r, is given by $\tau_r = N_{DXS} \cdot \tau_{event}$ (Table 3). We also calculate a total recurrence time for all the sources as a class using the total T_{obs} for all clusters (which gives the total τ_{event}) and the total N_{DXS} of 15. Figure 3c is plot of τ_r vs L_{min} for the four clusters. Recurrence times for sources in the clusters are constrained to lie above the lines. It is clear that with increasing event luminosity, T_{obs} increases and therefore τ_r increases, giving a tighter recurrence time constraint at higher luminosities. Table 3 displays recurrence time lower limits for event luminosities of 5×10^{35} and 1×10^{36} erg s^{-1}. The estimates of N_{DXS} are taken from the literature: 47 Tuc (Hasinger, Johnston and Verbunt 1994), NGC 5139 (ωCen) (Cool et al. 1995a), NGC 6397 (Cool et al. 1993), and NGC 6752 (Grindlay 1993b). For 47 Tuc we take only the DXSs within the core. For the latter three clusters we have assumed, for consistency, that sources within 5 core radii of each cluster center are associated with the GC and others are not. Note that changing N_{DXS} simply scales the numbers in Table 3 and the curves in Figure 3c.

These recurrence time limits can be compared to the several recurrent transients that have been discovered with all-sky X-ray surveys. One such transient is Aql X-1, observed over a 7 year period with the Vela 5B satellite. It has an outburst recurrence time measured at 1.2 years (Priedhorsky and Terrell 1984). Another example is Cen X-4 from which hard X-ray outbursts were observed in 1969 and 1979 (Kaluzienski, Holt and Swank 1980, Bouchacourt et al. 1984), indicating that its recurrence time is approximately 10 years or less, putting it at the outer edge of our limit. Both Aql X-1 and Cen X-4 have exhibited hard X-ray emission during outburst in excess of 1×10^{36} erg s^{-1} ($20 - 120$ keV) (c.f. Table 1). A number of other sources have also displayed recurrent outbursts: 1608-522, 1630-472, 1730-335 (Van Paradijs and Verbunt 1984, Chen, Shrader and Livio 1996). These systems have recurrence times of approximately 0.5 to a few years.

Our recurrence limits indicate that tran-

Cluster	D (kpc)	N_{DXS}	T_{obs} (years) 5×10^{35} erg s^{-1}	τ_r (years)	T_{obs} (years) 1×10^{36} erg s^{-1}	τ_r (years)
47 Tuc	4.6	5	2.0	3.4	3.5	5.8
NGC 5139	5.2	2	0.6	0.4	2.9	1.9
NGC 6397	2.2	5	3.6	6.0	3.6	6.0
NGC 6752	4.1	3	3.2	3.2	3.6	3.6
Total			9.4	13.0	13.6	17.4

Table 3: Recurrence time limits for the GCs in Search I. T_{obs} are the integrated times per cluster during which events of the specified luminosity would be detectable. τ_r are the corresponding maximum recurrence time of outbursts from the dim X-ray sources (DXSs). N_{DXS} are the estimated number of known DXSs in each cluster.

sient sources with outburst luminosities greater than approximately 1×10^{36} erg s^{-1} ($20 - 120$ keV) and recurrence times less than about 2 to 6 years cannot constitute the population of dim GC sources in the four sampled clusters. The recurrence time lower limit for all sources is ~ 20 years, if one is willing to consider them as a class. This suggests that the dim sources in these clusters are not quiescent LMXBs of a type similar to Aql X-1 or Cen X-4. Some caution should be taken with this interpretation. The outburst recurrence times are determined well only for a few systems which may not be typical. Also LMXBs in GCs may have systematically different properties than the field binaries in which the hard X-ray emission and recurrent outbursts have been observed. Indeed some bright LMXBs in GCs have unusual properties, for example very short orbital periods (Bailyn 1996). One might argue that a substantial number of X-ray outbursts from Aql X-1-like LMXBs might be detectable only below 20 keV. If this were the case, such events would be not detectable by BATSE. However, the recently monitored behavior of Aql X-1 shows clearly that BATSE can usually detect hard X-ray emission at times when the optical counterpart of Aql X-1 is excited. These events are most likely associated with major X-ray outbursts (Harmon et al. 1996).

6. Limits from the Persistent Emission Search

We have searched for longer time scale persistent emission using the flux histories for the four GCs in Search B. Previous upper limits have been obtained only for 47 Tuc. Observations with SIGMA spanning seven days set a limit at $\sim 2 \times 10^{35}$ erg s^{-1} ($40 - 100$ keV) (Barret et al. 1993) and an observation by the balloon-borne EXITE instrument found an upper limit of 1.4×10^{36} erg s^{-1} ($30 - 150$ keV) (Grindlay et al. 1993c). Upper limits have also been obtained for 47 Tuc with COMPTEL, OSSE and EGRET in their respective bands (O'Flaherty et al. 1995).

Our BATSE search offers improved sensitivity as a result of the very long integration time. We have detected no emission for the four clusters. The upper limits are summarized in Table 4. We have obtained these upper limits by formal error calculations integrating over large time windows. As discussed in Section 3, such a procedure yields error val-

Cluster	F_{ul} (γ cm^{-2}s^{-1}) [$\times 10^{-4}$]	L_{ul} (erg s^{-1}) [$\times 10^{34}$]	N_{isol}	F_{inter} (γ cm^{-2}s^{-1}) [$\times 10^{-5}$]	N_{inter}
47 Tuc	3.3	5.8	19	0.71	46
NGC 5139	4.1	9.2	31	0.62	66
NGC 6397	4.2	1.7	6	3.10	14
NGC 6752	3.6	5.0	17	0.85	42

Table 4: Persistent emission upper limits for GCs in Search I. The table lists F_{ul} (values are $\sim$1 mCrab), the 2σ flux upper limits ($20-120$ keV), L_{ul}, the corresponding luminosity upper limits for power law spectra with index 2, N_{isol}, the maximum number of isolated MSPs producing hard X-ray emission based on the model of Chen (1991), F_{inter}, the estimated flux produced by a single interacting MSP, and N_{inter}, the maximum number of interacting binary MSPs for an assumed pulsar spin-down power of 10^{34} erg s^{-1} (Tavani 1993b).

ues systematically larger than the actual flux distribution. We have studied this effect for the four GCs of Search B and determined a correction factor of 1.6 based on fitted widths of flux distributions. We have used the factor of 1.6 correction to the formal error estimates for the upper limit values of Table 4. The clusters of Search B were chosen to limit the systematic effects of interfering sources, a selection which permits very sensitive flux limits. We note that the sensitivities may depend on the assumed spectral shape used in deconvolution. We have employed power law spectra with photon index 2.0.

Using our upper limits, we constrain the number of isolated high energy emitting MSPs in the clusters. The luminosity for a typical non-interacting MSP can be calculated. Chen (1991) does this using the outer-gap emission model of Cheng, Ho and Ruderman (1986) and the observed period distribution for MSPs. The resulting luminosity from a cluster is a constant times the number of isolated MSPs, assuming isotropic emission. For a cluster with one MSP, this would yield a luminosity of approximately 3×10^{33} erg s^{-1}. Combining this luminosity estimate with our luminosity upper limit, we find the maximum number of isolated MSPs, N_{isol}, in each of the clusters (Table 4). The estimate of N_{isol} depends on the period distribution of MSPs. In the luminosity calculation, Chen (1991), uses the period distribution of all the 28 then-known MSPs, fit as a falling power law. This distribution is poorly constrained due to selection effects and small number statistics and may vary from cluster to cluster. This adds additional uncertainty to our values of N_{isol}.

The flux from an interacting binary MSP has been estimated by Tavani (1993b). Using this model we calculate the estimated flux from each cluster for a single interacting MSP system, F_{inter} (Table 4). Combined with our flux upper limits, the flux estimate yields an upper limit on the number of interacting MSPs, N_{inter}. The constraints on N_{inter} are weak. This calculation uses an average MSP spin-down power of 10^{34} erg s^{-1} (Taylor et al. 1995). MSP spin-down powers are in the range 10^{33}-10^{36} erg s^{-1} but are still not well constrained.

7. Conclusions

We have monitored 27 galactic globular clusters (GCs) with BATSE during a period of approximately four years each. We have detected no distinct hard X-ray outburst episodes and no persistent emission. The lack of detected events has several interesting implications.

For the GCs with dim X-ray sources (DXSs), we find a lower limit for the outburst recurrence time from DXSs of $\tau_r \sim 2 - 6$ years. This limit excludes the existence of 'Aql X-1-like' objects (i.e., persistent X-ray sources subject to major X-ray outbursts with a time scale of ~ 1 year), since τ_r is comparable to or greater than this outburst recurrence time scale. This suggests that the DXSs in these clusters are not LMXBs similar to Aql X-1.

The lack of strong outburst events in our search means we also have no evidence of accreting BHs in GCs. If active BH binaries exist in GCs, they would be clearly detectable with hard X-ray luminosities of order of $10^{36} - 10^{37}$ erg s^{-1}.

We have calculated upper limits on persistent hard X-ray emission from GCs. The limiting luminosity is $\sim (2-10) \times 10^{34}$ erg s^{-1} for the closest clusters. The limit for 47 Tuc is somewhat more sensitive than previous measurements. A model-dependent but reasonable estimate of the expected hard X-ray magnetospheric emission from isolated MSPs (Chen 1991) implies that the number of isolated MSPs emitting hard X-rays in 47 Tuc is less than 19. Taking the observed 11 MSPs in 47 Tuc, and a beaming factor of 2 for short period pulsars, this upper limit is comparable to actual number of MSPs in 47 Tuc. Our results are therefore a constrain the magnetospheric model of MSP hard X-ray emission.

Our upper limits on persistent hard X-ray emission also provide a mild constraint on the number of interacting pulsars in binaries. The observed efficiency (a few percent) of conversion of pulsar spindown luminosity into hard X-ray emission in the case of the periastron passage of the Be star/pulsar system PSR B1259-63 (Tavani et al. 1996, Grove et al. 1995) together with the observed MSP spindown average luminosity of 10^{34} erg s^{-1} implies a limit to the GC population interacting pulsar binaries. We find limits of $14 - 66$ interacting MSPs in the clusters studied.

We would like to acknowledge the BATSE instrument team for their support. We thank Jonathan Grindlay, Didier Barret and Andrew Chen for helpful comments. We thank Mark Stollberg for assistance with data analysis. This work is Columbia Astrophysics Laboratory Contribution Number 596. This work is supported in by NASA Grants NAG 5-2235 and NGT 8-52806.

REFERENCES

Bahcall, J. and Ostriker, J. 1975, Nature, 256, 23

Bailyn, C. 1996, in The Origins, Evolution, and Destinies of Binary Stars in Clusters, eds. E.F. Milone and J.C. Mermilliod, (ASP Conf. Ser.), in press

Bailyn, C. 1995, ARAA, 33, 133

Barret, D. and Grindlay, J. 1995, ApJ, 440, 841

Barret, D. et al. 1996, in 3rd Compton Symposium, Munich, in press

Barret, D. and Vedrenne, G. 1994, ApJS, 92, 505

Barret, D. et al. 1993, ApJ, 405, L59

Barret, D. et al. 1992, ApJ, 394, 615

Barret, D. et al. 1991, ApJ, 379, L21

Bouchacourt, P. et al. 1984, ApJ, 285, L67

Chen, K. 1991, Nature, 352, 695

Chen, K., Middleditch, J. and Ruderman, M. 1993, ApJ, 408, L17

Chen, W., Shrader, C., and Livio, M. 1996, ApJ, submitted

Cheng, K.S., Ho, C., and Ruderman, M. 1986, ApJ, 300, 500

Churazov, E., et al. 1995, ApJ, 443, 341

Churazov, E., et al. 1994, Adv. in Space Res., COSPAR, Munich, in press

Clark, G.W. 1975, ApJ, 199, L143

Cool, A.M. et al. 1995a, ApJ, 438, 719

Cool, A.M. et al. 1995b, ApJ, 439, 695

Cool, A.M. et al. 1993, ApJ, 410, L103

Forman, W., Jones, C. and Tananbaum, H. 1976, ApJ, 207, L25

Grindlay, J.E. 1993a, Adv. Space Res., 13(12), 597

Grindlay, J. 1993b, in Dynamics of Globular Clusters - eds. S. Djorgovski and G. Meylan (ASP Conf. Ser.), 285

Grindlay, J. et al. 1993c, in Compton Gamma-Ray Observatory, AIP Conf. Proc. 280, eds. M.Friedlander, N.Gehrels and D. Macomb, (New York:AIP), 243

Grove, J.E., et al. 1995, ApJ, 447, L113

Harmon, B.A. et al. 1996, in 3rd Compton Symposium, Munich, in press

Harmon, B.A., et al. 1992, Compton Observatory Science Workshop, NASA CP 3137, 69

Hasinger, G., Johnston, H.M., and Verbunt, F. 1994, A&A, 288, 466

Hertz, P. and Grindlay, J. 1983, ApJ, 275, 105

Hertz, P. and Wood, K.S. 1985, ApJ, 290, 171

Hut, P. et al. 1992, PASP, 104, 981

Kulkarni, S.R., Hut, P. and McMillan, S. 1993, Nature, 364, 421

Kaluzienski, L.J., Holt, S.S., and Swank, J.H. 1980, ApJ, 241, 779

Kluzniak, W. et al. 1988, Nature, 334, 225

A. Lyne, 1996, in Proc. 7th M. Grossmann Symposium, eds. M. Kaiser, R. Jantzen, (World Scientific), in press

Margon, B. and Bolte, M. 1987, ApJ, 321, L61

Mereghetti, S. et al. 1995, A&A, 302, 713

Mitsuda, K. et al. 1989, PASJ, 41, 97

O'Flaherty, K.S., et al. 1995, A&A, 297, L29

Pendleton, G.N. et al. 1996, NIM, in press

Peterson, C.J. 1993, in Structure and Dynamics of Globular Clusters: ASP Conf. Proc. Vol. 50, eds. S.G.Djorgovski and G. Meylan (SanFrancisco:ASP), 337

Priedhorsky, W.C. and Terrell 1984, ApJ, 280, 661

Pye, J. and McHrady, I. 1983, MNRAS, 205, 875

Robinson, C. et al. 1995, MNRAS, 274, 547

Ruderman, M. and Cheng, K.S. 1988, ApJ, 335, 306

Tanaka, Y. and Lewin, W.H.G. 1995 in X-Ray Binaries, eds. W.H.G.Lewin, J.van Paradijs, and E.P.J. van den Heuvel (Cambridge University Press), 126

Tanaka, Y. 1989, in Proc. of the 23rd ESLAB Symposium, Vol. 1, ed. J.Hunt (ESA Pub. Div.), 3

Tavani M., et al., 1996, A&AS, in press

Tavani, M. 1993a, AAS, 97, 313

Tavani, M. 1993b, ApJ, 407, 135

Tavani, M. 1991, ApJ, 379, L69

Tomaney, A., Crotts, A., and Shafter, A. 1994, BAAS, 181, 73.09

Taylor, J. et al. 1995, Princeton Pulsar Catalog

Van Paradijs, J. and Verbunt, F. 1984, in High Energy Transients in Astrophysics, ed. S.E. Woosley (New York: AIP), 49

Verbunt, F., van Paradijs, J., and Elson, R. 1984, MNRAS, 210, 899

Verbunt, F., et al. 1994, MmSAI, 65, 249

Verbunt, F., et al. 1995, A&A, 300, 732

White, N.E., Kaluzienski, J.L., and Swank, J.H. 1984, in High Energy Transients in Astrophysics, ed. S.E. Woosley (New York: AIP), 31

Zhang, S.N. 1996, in 3rd Compton Symposium, Munich, in press

Zhang, S.N., et al. 1993, Nature, 366, 245

This 2-column preprint was prepared with the AAS LaTeX macros v4.0.

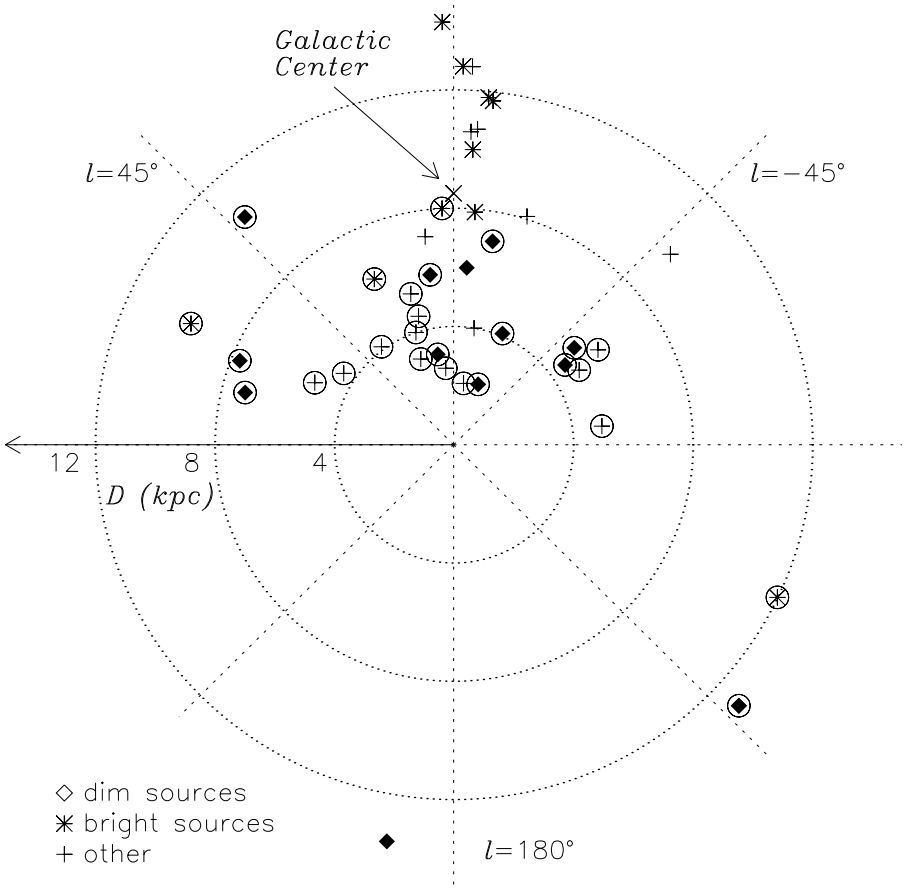

Fig. 1a.— Projection of the positions of globular clusters onto the galactic plane. All the circled clusters are included in our Search A or Search B.

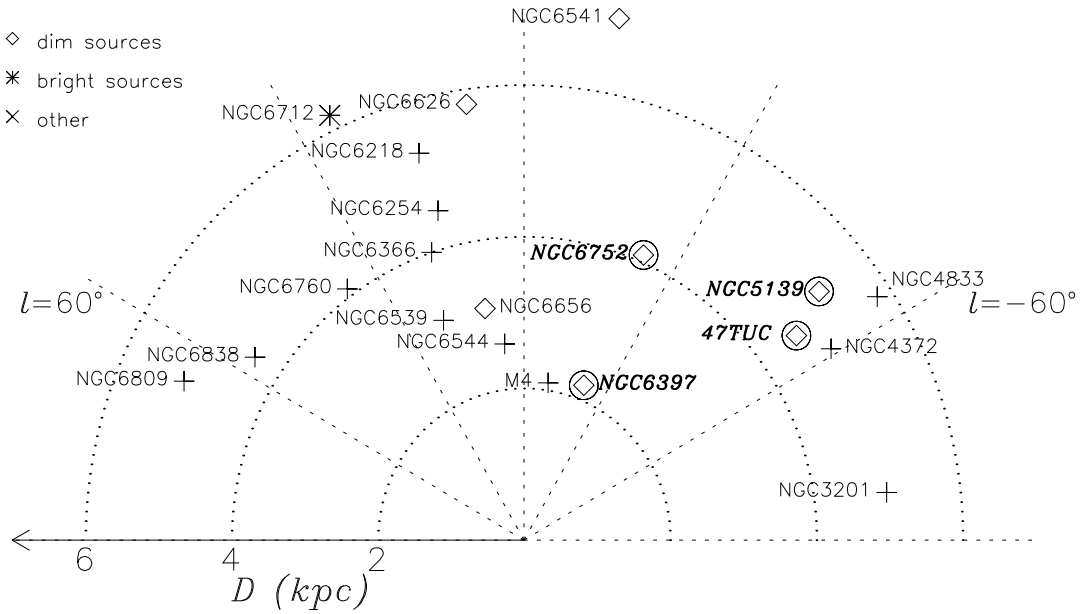

Fig. 1b.— Globular clusters within 6 kpc projected onto the plane. The four clusters for which we have performed the sensitive Search B are circled. All the other clusters are included in Search A.

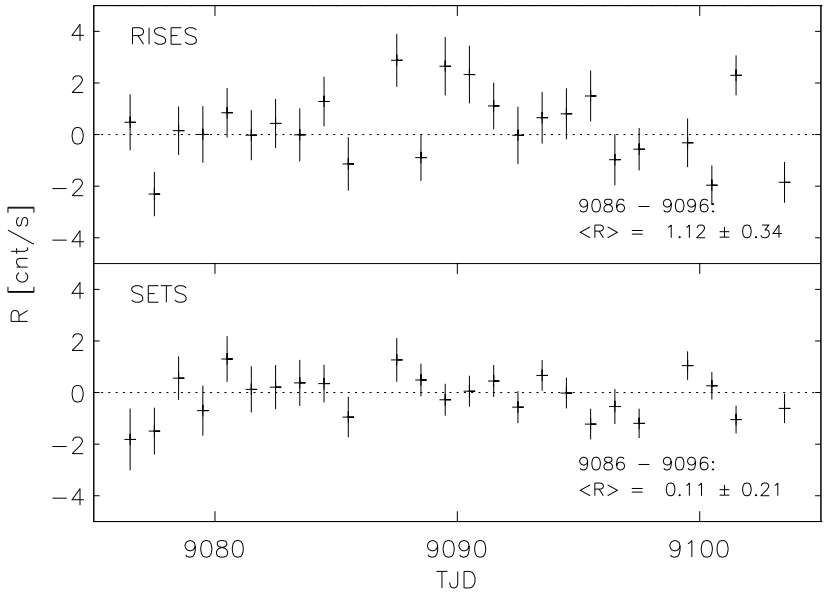

Fig. 2a.— Rate histories during candidate event in NGC 6752 near TJD 9090. The rate histories have been separated into rise and set rates, and corrected approximately for detector response. The average rise and set rates during the approximate time of the event are shown.

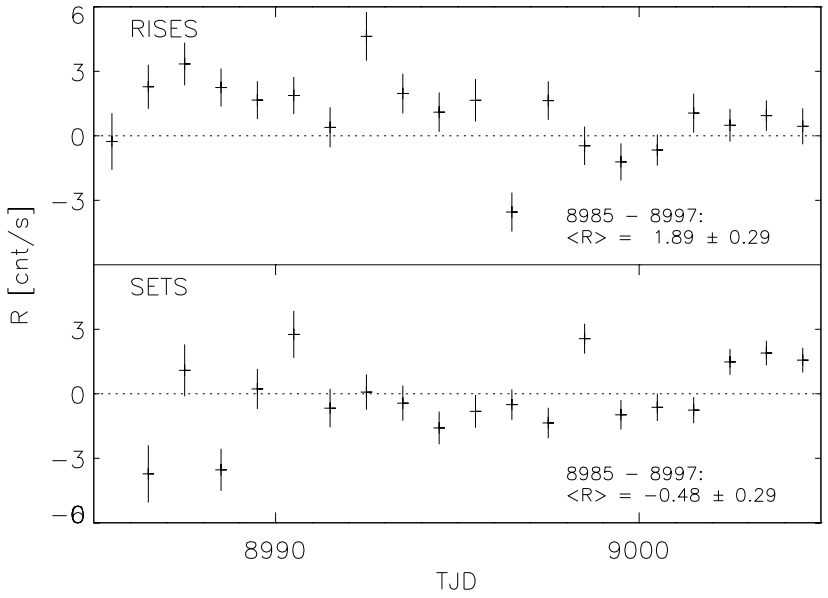

Fig. 2b.— Rate histories during candidate event in NGC 5139 near TJD 8990.

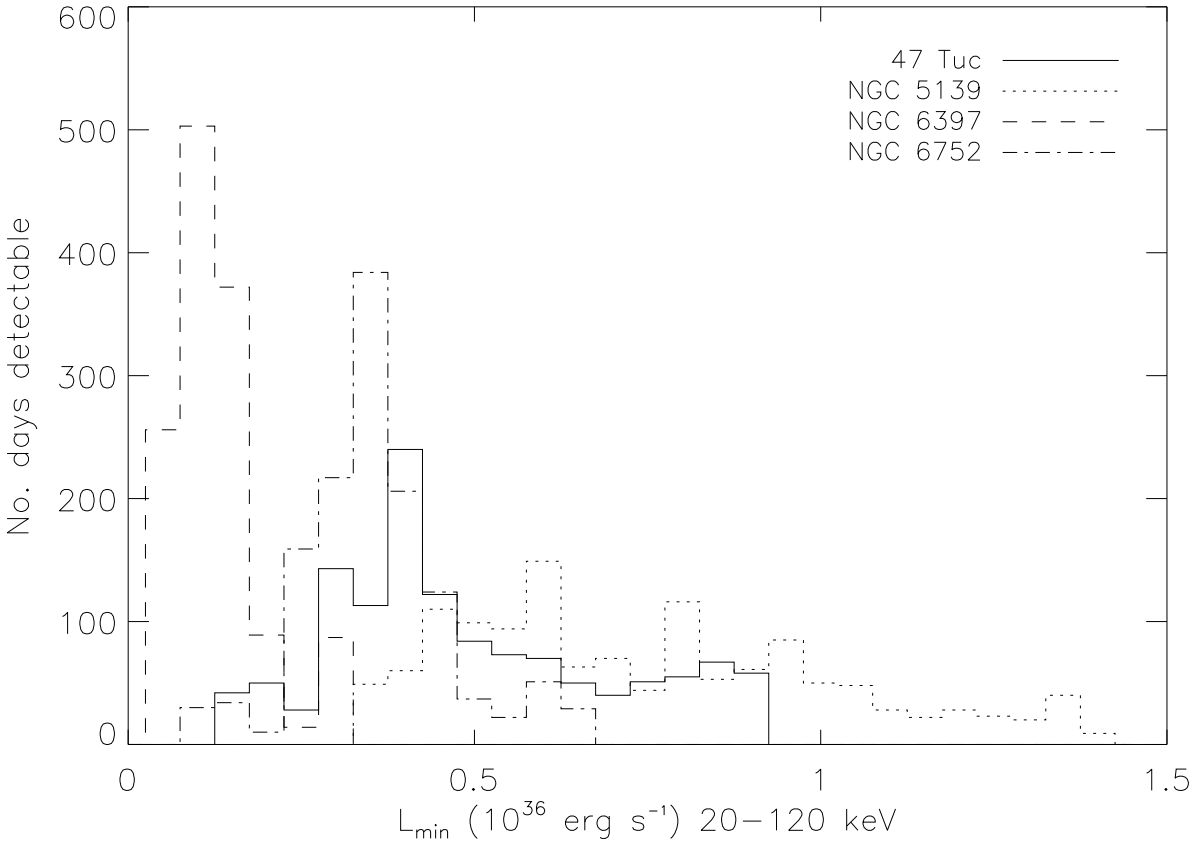

Fig. 3a.— Coverage for the four clusters of Search A. Data integration time is 10.0 days.

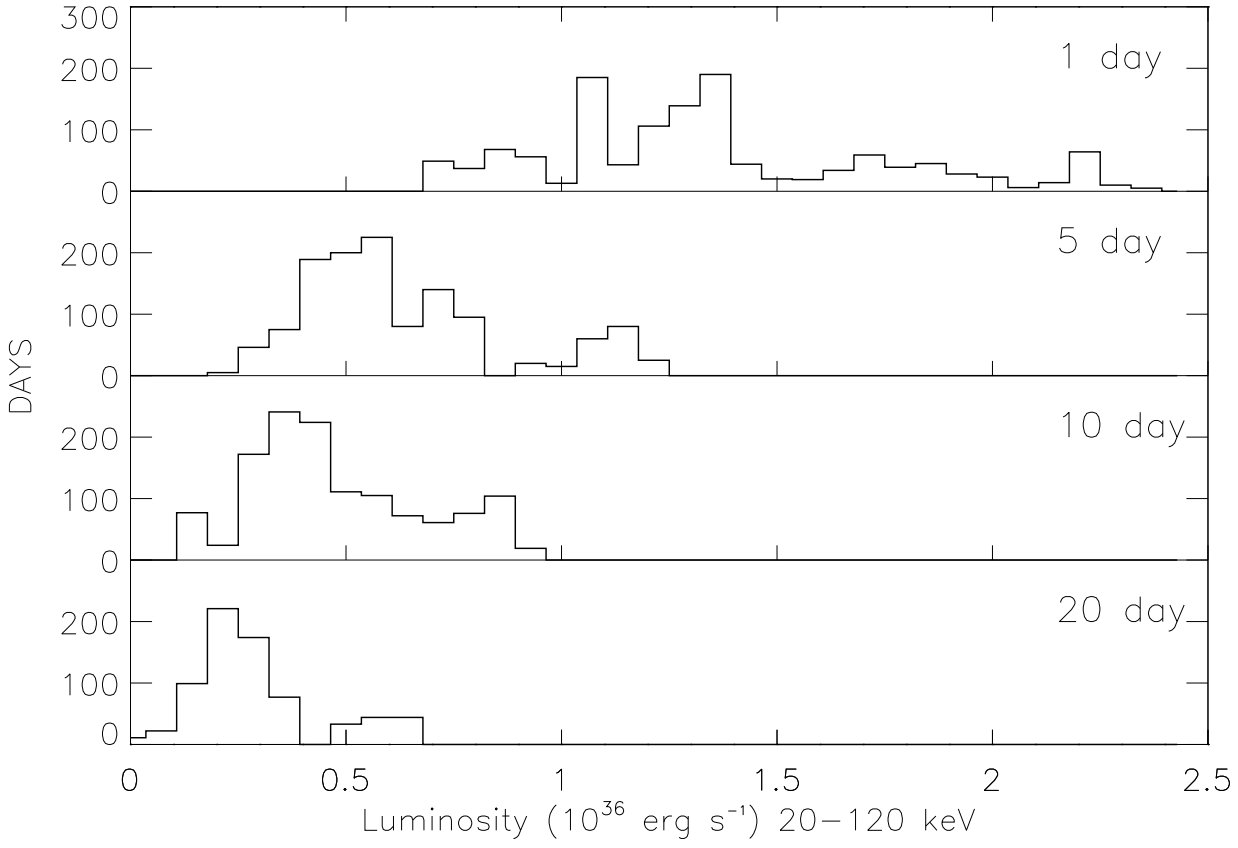

Fig. 3b.— Coverage for the cluster 47 Tuc using various data integration times.

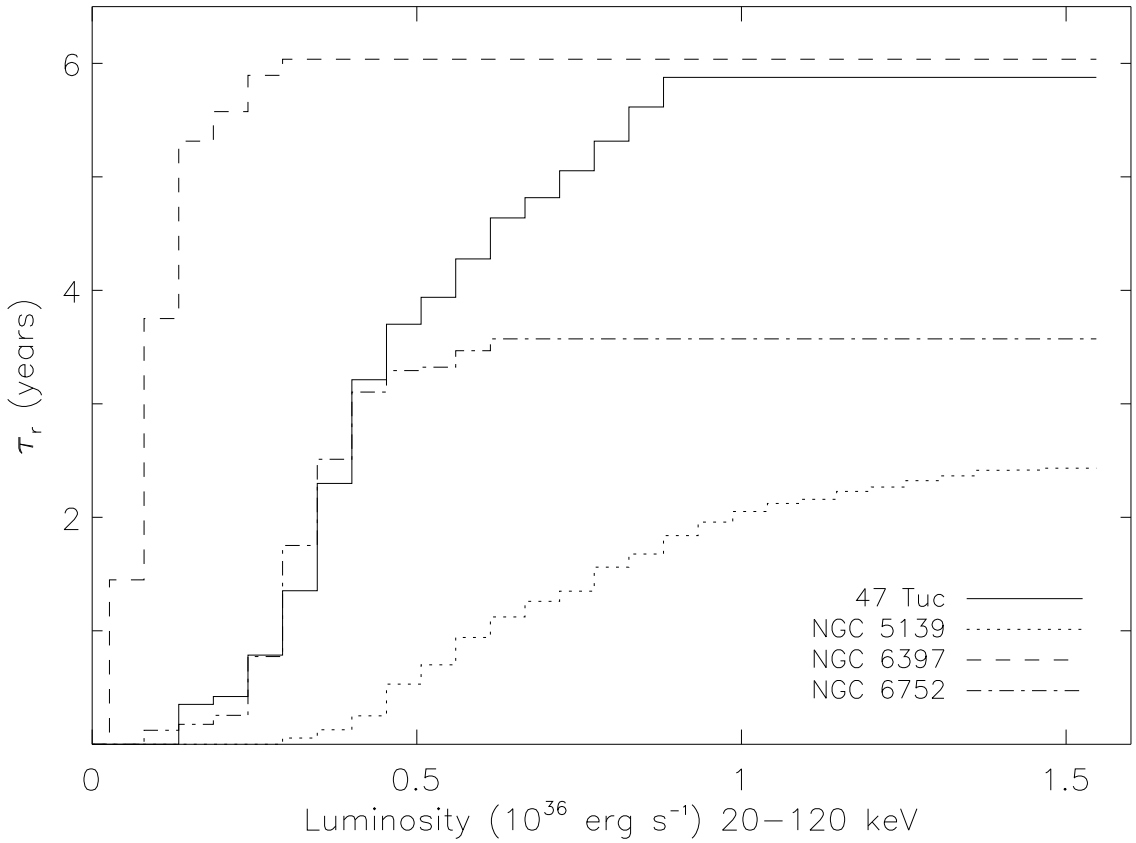

Fig. 3c.— Recurrence time lower limits for dim X-ray sources. Recurrence times are constrained to lie above the curves. A data integration time of 10.0 days has been used.